AD-A157 434 ANALYSIS OF ARCTIC HAZE SCATTERING AND AEROSOL DATA OBTAINED DURING AGASP.. (U) GEORGIA INST OF TECH ATLANTA SCHOOL OF GEOPHYSICAL SCIENCES E M PATTERSON ET AL. 1/1

UNCLASSIFIED 01 MAY 85 ARO-21001.1-GS DAAG29-83-K-0163 F/G 20/6 NL

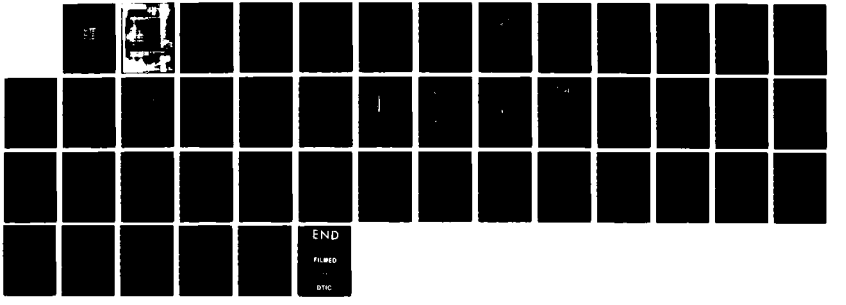

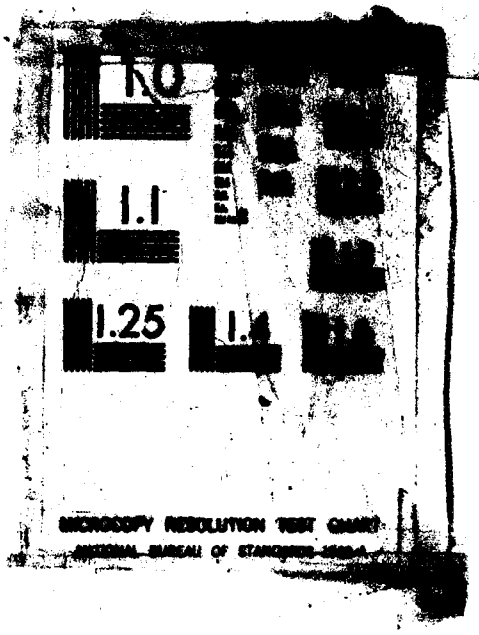
1.1
1.25
MICROCOPY RESOLUTION TEST CHART

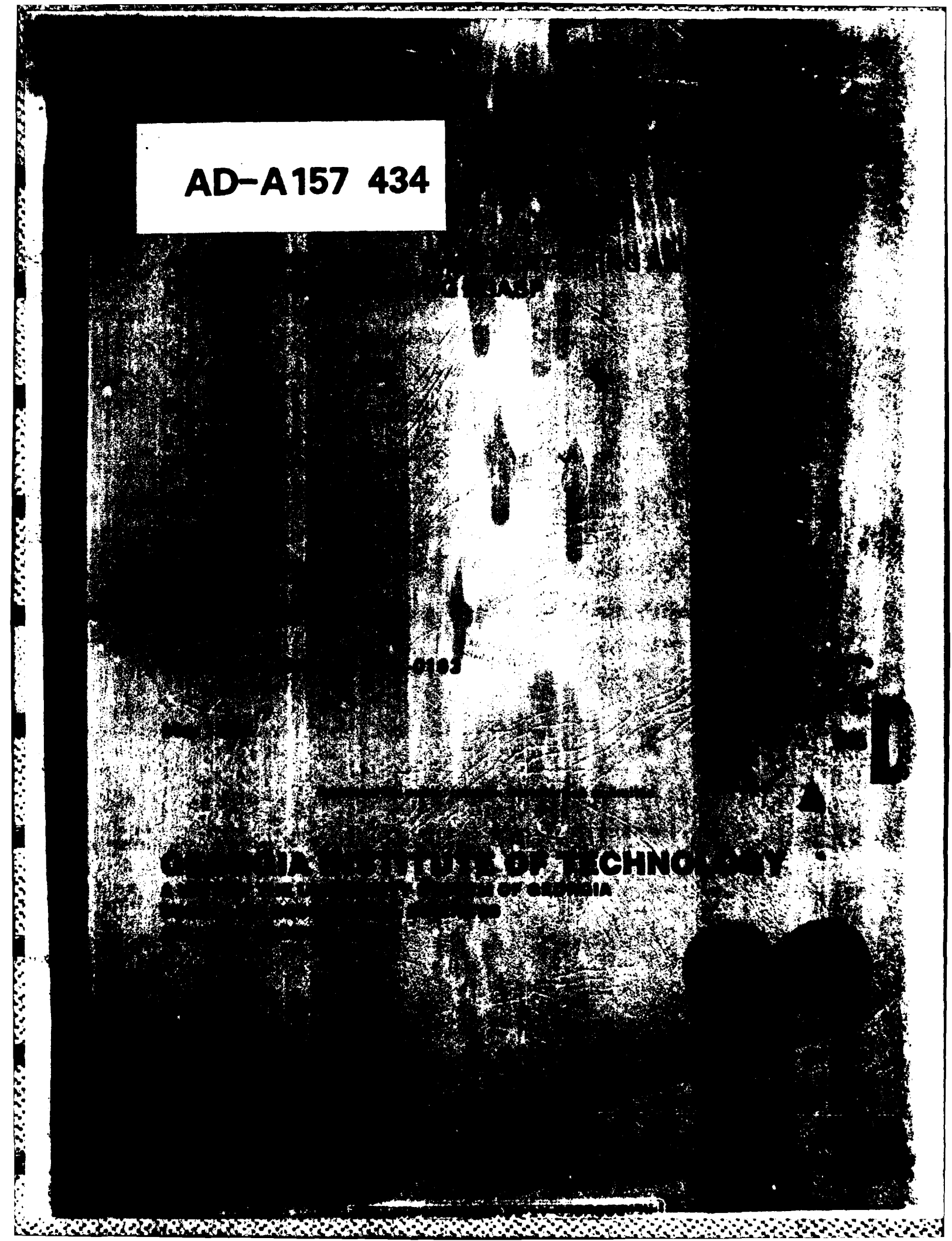

SECURITY CLASSIFICATION OF THIS PAGE (When Data Entered)

REPORT DOCUMENTATION PAGE

READ INSTRUCTIONS BEFORE COMPLETING FORM

1. REPORT NUMBER: ARO 21001.1-GS	2. GOVT ACCESSION NO.: AD-A157434
3. RECIPIENT'S CATALOG NUMBER	
4. TITLE (and Subtitle): Analysis of Arctic Haze Scattering and Aerosol Data Obtained During AGASP	5. TYPE OF REPORT & PERIOD COVERED: FINAL 9/16/83 - 9/15/84
6. PERFORMING ORG. REPORT NUMBER	
7. AUTHOR(s): E. M. Patterson, G. W. Grams	8. CONTRACT OR GRANT NUMBER(s): DAAG 29-83-K-0163
9. PERFORMING ORGANIZATION NAME AND ADDRESS: School of Geophysical Sciences, Georgia Institute of Technology, Atlanta, Georgia 30332-0340	10. PROGRAM ELEMENT, PROJECT, TASK AREA & WORK UNIT NUMBERS
11. CONTROLLING OFFICE NAME AND ADDRESS: U. S. Army Research Office, Post Office Box 12211, Research Triangle Park, NC 27709	12. REPORT DATE: May 1, 1985
	13. NUMBER OF PAGES
14. MONITORING AGENCY NAME & ADDRESS (if different from Controlling Office)	15. SECURITY CLASS. (of this report): UNCLASSIFIED
	15a. DECLASSIFICATION/DOWNGRADING SCHEDULE

16. DISTRIBUTION STATEMENT (of this Report)

Approved for public release; distribution unlimited.

17. DISTRIBUTION STATEMENT (of the abstract entered in Block 20, if different from Report)

N/A

18. SUPPLEMENTARY NOTES

THE VIEW, OPINIONS, AND/OR FINDINGS CONTAINED IN THIS REPORT ARE THOSE OF THE AUTHOR(S) AND SHOULD NOT BE CONSTRUED AS AN OFFICIAL DEPARTMENT OF THE ARMY POSITION, POLICY, OR DECISION, UNLESS SO DESIGNATED BY OTHER DOCUMENTATION.

19. KEY WORDS (Continue on reverse side if necessary and identify by block number)

AGASP measurements, Arctic haze, scattering aerosol measurements, aerosol size distributions

20. ABSTRACT (Continue on reverse side if necessary and identify by block number)

We have analyzed polar nephelometer scattering data to infer radiative parameters for the Arctic haze aerosols. We have also used the scattering properties as measured with the nephelometer as well as other measurements of aerosol microphysical properties to improve our estimates of aerosol properties for radiative modeling. We have confirmed earlier estimates of the submicron size distribution and have demonstrated the uniformity of these distributions. We have also shown that the giant particles also have relatively uniform size distributions and have provided an estimate of the infrared effects due to these particles.

DD FORM 1 JAN 73 1473 EDITION OF 1 NOV 65 IS OBSOLETE

SECURITY CLASSIFICATION OF THIS PAGE (When Data Entered)

ANALYSIS OF ARCTIC HAZE SCATTERING AND AEROSOL DATA OBTAINED DURING ACASP

FINAL REPORT

E. M. PATTERSON AND G. W. GRAMS

1 MAY 1985

U.S. ARMY RESEARCH OFFICE

CONTRACT NUMBER DAAG29-83-K-0163

SCHOOL OF GEOPHYSICAL SCIENCES
GEORGIA INSTITUTE OF TECHNOLOGY
ATLANTA, GA 30332

APPROVED FOR PUBLIC RELEASE;
DISTRIBUTION UNLIMITED.

Table of Contents

1. INTRODUCTION

In our initial plan of work, we divided our efforts into two areas:

1) Analysis of the Georgia Tech polar nephelometer data; and

2) Analysis of the scattering data from our nephelometer and the other light scattering instruments in relation to the other aerosol measurements to provide information that is needed to model the radiative effects of the Arctic haze. Our final report, which is structured in a similar fashion, consists of a section describing the AGASP experiment, a section describing the Georgia Tech polar nephelometer results, a section describing our general analysis for modeling purposes, and a concluding section.

2. AGASP EXPERIMENT

The Arctic Gas and Aerosol Sampling Program (AGASP) was conducted across the Arctic in the spring of 1983 to study the large scale air pollution phenomenon known as Arctic haze. The aircraft measurement component of this program utilized a National Oceanic and Atmospheric Administration WP-3D Orion research aircraft to study the haze in-situ and to extend into three dimensions the Arctic haze measurements conducted at the various surface stations in the Arctic.

The AGASP program (described by Schnell, 1984) was a multifaceted program which included the following aerosol measurement objectives: 1. Determination of aerosol size spectra, optical properties, chemical composition, distribution and trajectories; 2. Measurements of both in-situ and surface observed radiative effects of the haze. The aircraft aerosol instrumentation included several aerosol samples, a condensation nucleus counter, two PMS (Particle Measuring System) aerosol spectrometer probes for particle sizing, a NOAA integrating nephelometer, and the Georgia Tech polar nephelometer.

Flight tracks of the NOAA WP-3D during the AGASP project are shown in Figure 2.1 which is taken from Schnell (1984).

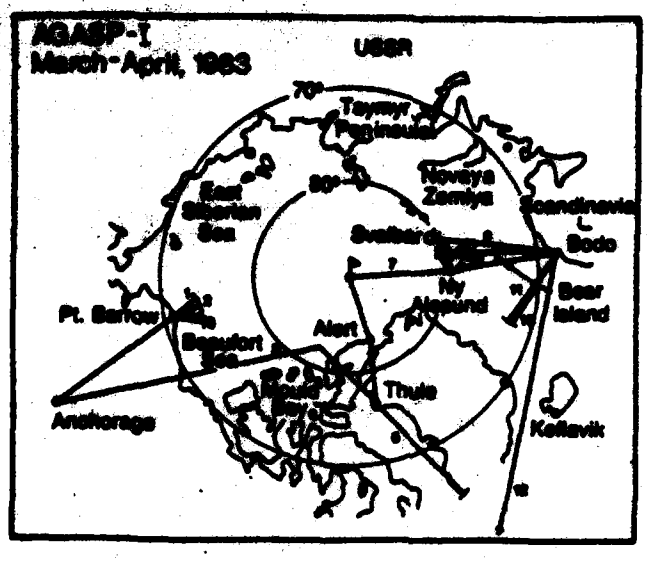

Fig. 2.1 Approximate flight tracks of the NOAA WP-3D during the AGASP project. Data from flights 1 (3-11-83), 2 (3-13-83), 3 (3-15-83), and 8 (3-31-83) are discussed in this report (from Schnell, 1984).

3. POLAR NEPHELOMETER MEASUREMENTS

The Georgia Tech polar nephelometer was designed to measure the total aerosol scattering and the scattering as a function of angle, from which the scattering phase function and asymmetry parameter may be determined.

The basic concept of the Georgia Tech polar nephelometer can be explained with reference to the device described by Grams et al. (1975). The general features of the instrument are shown in Figure 3.1. A collimated laser beam serves as the light source and the detector optical system defines a narrow field of view (0.5° half angle). The photon counting system measures photomultiplier pulse rates with the light beam on and off, with the differences in the measured pulse rate being directly proportional to the intensity of the light scattered from the volume common to the intersection of the laser beam and the detector field of view. Measurements are made at different scattering angles by rotating the detector relative to the direction of propagation of the laser beam.

Earlier Georgia Tech measurements with polar nephelometers have included a ground-based study to determine the complex index of refraction of airborne soil particles (Grams et al., 1974), a series of airborne observations of the optical properties of aerosols in the troposphere and lower stratosphere (e.g., Grams, 1981), and laboratory experiments on the optical properties of airborne particles as a function of their size, shape and refractive index (e.g., Grams and Coletti, 1981).

As part of the NASA Aerosol Climate Experiment (ACE), a new version of this instrument was developed to be mounted and flown on one of NASA's U2 aircraft. This effort was initiated approximately 5 years ago as part of a NASA special study which, in conjunction with satellite observations and

other related aerosol programs, was designed to provide comprehensive data sets and analytical capabilities for evaluating the impact of stratospheric aerosol particles on the Earth's climate, for testing climate models by studying the properties and effects of a large volcanic eruption, and for determining the influence of aerosols on remote sensing techniques.

The new design evolved from our efforts to satisfy the limitations that were placed on the size, weight, and power consumption of the instrument for operation on the U-2 aircraft. The elimination of moving parts (such as the rotating detector system in the original nephelometer) also proved to be highly desirable for aircraft operations. We therefore designed a system for measuring the amount of light scattered by aerosol particles as a function of angle relative to the direction of a collimated Helium-Neon laser beam by operating an image-intensified scanned-diode array in the focal plane of a wide-angle "fisheye" lens. A schematic of this arrangement is shown in Figure 3.2.

The light scattered from the narrow collimated laser beam by atmospheric molecules and aerosol particles is focused along a line parallel to the source beam in the focal beam of the lens. The linear diode-array detector is positioned to measure the light intensity along that line. With the 180° wide-angle lens focused at infinity, each point along the array corresponds to a discrete scattering angle. The diode array simultaneously measures the amount of light incident on each of 512 different positions along the line. The practical limits on the angular range of the instrument are for scattering angl' from about 5° to 175° from the direction of the source beam. In the focal plane of the lens, this angular limit transforms approximately to the middle 400 elements of the diode array and we thereby have an angular resolution of approximately 0.5°.

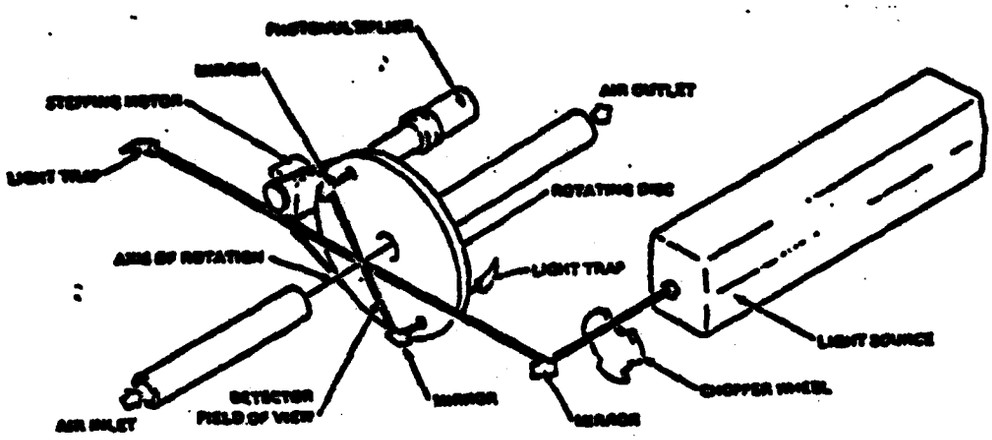

Fig. 3.1. Schematic illustration of the Georgia Tech laser polar nephelometer (from Grams, Dascher, and Wyman, 1975).

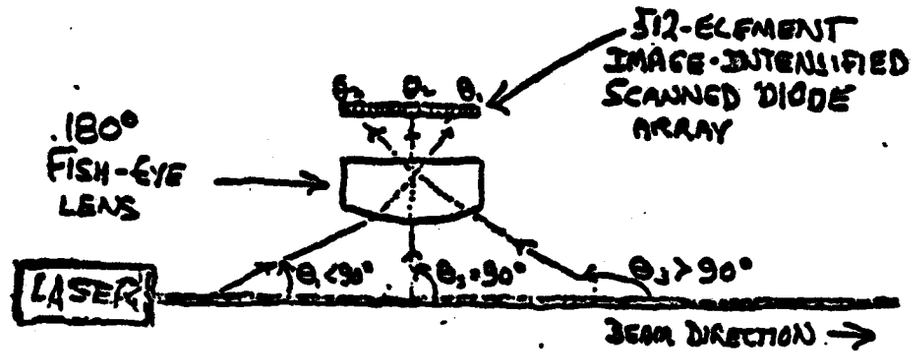

Fig. 3.2. Schematic illustration of the optical configuration of the Georgia Tech laser polar nephelometer developed for operation on the NASA U-2 aircraft. Light scattered from a laser beam by air molecules and aerosol particles is focussed by a 180° wide-angle fisheye lens to a line in the focal plane of the lens that is parallel to the beam direction. Light from different angles is focussed to different points along that line. An image-intensified scanned linear diode array is positioned to record the scattered light intensity at each angle. In the figure, the symbol θ_1 is used to depict a forward scattering angle and θ_3 backscattering; θ_2 depicts light scattered normal to the beam direction. See text for more details.

The signals recorded by all of the elements of the detector array are periodically read by a microprocessor based data management system. This system controls the operation of the instrument and records data using a Digital Equipment Corporation LSI-11/23 microprocessor with 64 Kbytes of memory with a disk operating system based on a 19 Mbyte Winchester disk drive. The disk recording system is used to store the instrument control and data analysis programs and, also, to record the large amounts of data read from the detector array.

The laser beam used in the nephelometer is linearly polarized. A disk in the path of the laser beam can be rotated to 3 different positions by a small motor. One position blocks the beam so that a background signal without the presence of the source beam can be established. The second position is a circular hole in the disk which allows the linearly polarized laser beam to illuminate the volume being sampled; the location of the detector system is designed to allow us to observe the polar distribuiton of light scattered in the plane that is perpendicular to the direction of the electric vector of the source beam. A half-wave plate has been mounted at the third position; this optical element rotates the original plane of polarization of the laser beam by 90 degrees so that the detector system measures the polar diagram for the parallel scattering plane. Each nephelometer scan consists of the signals recorded by each of the 512 elements of the detector array for the 3 different positions of the disk. The sample time required to complete each 3-part scan can vary from just a few seconds for use in conditions of heavy aerosol loading to longer time intervals for observations in high visibility conditions. To indicate the overall sensitivity of the system, we point out that integration times of approximately one minute are required to obtain observations of molecular scattering (without aerosol particles present)

when operating the instrument at U-2 sampling altitudes with ambient pressures of about 100 millibars.

The construction of the nephelometer was completed and the device was first flown in test flights on the NASA U-2 during October 1981 and April 1982. Our first data flights were made during July 1983. Additional stratospheric data were obtained during U-2 and ER-2 flights made in December 1982 and July 1983. With respect ot the current study, the nephelometer was also flown as part of the aerosol instrument package on the NOAA P-3 aircraft as part of the Arctic Gas and Aerosol Sampling Program (AGASP) study of Arctic haze layers (Schnell, 1984).

The potential for generating large amounts of data during field measurements that involve several 6-8 hour flights is clearly present with the instrument. For example, our U-2 flights provided us with almost 850 three part scans during the July 1982 flights, approximately 300 scans during the December 1982 flights and several hundred additional scans during the July 1983 flights. The Arctic haze observations during the AGASP flights in Spring 1983 provided almost 3000 more 3-part scans. A significant part of our data analysis effort has involved the development of procedures to present such large amounts of raw data in scientifically useful forms.

Our initial approach was that of preparing graphs or tables of scattering cross sections and scattering asymmetry parameters obtained by applying least-squares curve-fitting techniques to establish "best-fit" parameters for Henyey-Greenstein phase functions as described by Grams (1981). In support of qualitative "quick-look" applications, we also carried out some analytical studies showing that the amount of light detected by the polar nephelometer at scattering angles near 45° is approximately proportional (to within a factor of 2) to the total scattering cross section of the

aerosol particles. An example of a plot of 45° scattering cross section versus time as recorded by the laser nephelometer on a U-2 flight is shown in Figure 3.3. Data of this type were printed out in real time on the NOAA P-3 aircraft during the Spring 1983 AGASP flights to help establish the times that the aircraft was within a layer of Arctic haze.

During the past year, we initiated a comprehensive program for calibrating the nephelometer. Although the recording of data with the instrument could be (and was) accomplished without an absolute calibration of the instrument, we felt that our results could not be published until such calibrations had been completed. In some of our field observations, such as the AGASP Arctic haze flights, the real-time 45° output of the instrument, as illustrated in Figure 3.3, was used by the scientists aboard the aircraft as a means of determining when the aircraft was within a layer of haze particles. However, one of our major goals has been to obtain a more quantitative treatment of the data.

Perhaps the most difficult factor in relating the photon counts recorded by each channel of the diode array has been the extreme difficulty in establishing the exact proportion of the observed counts due to molecular scattering by the atmospheric volume being sampled. To illustrate the nature of the problem, the reader is referred to Figure 3.4 which is a published example of a polar nephelometer observation made by an earlier version of the Georgia Tech laser polar nephelometer system (Grams, 1981). While the figure refers to observations of light scattering by aerosol particles in the stratosphere, it is representative of the type of observations provided by our airborne nephelometer system.

The curves shown in the figure illustrate several important points. The first and most important point to be made is the fact that, except for the extreme forward directions, molecular scattering often dominates the

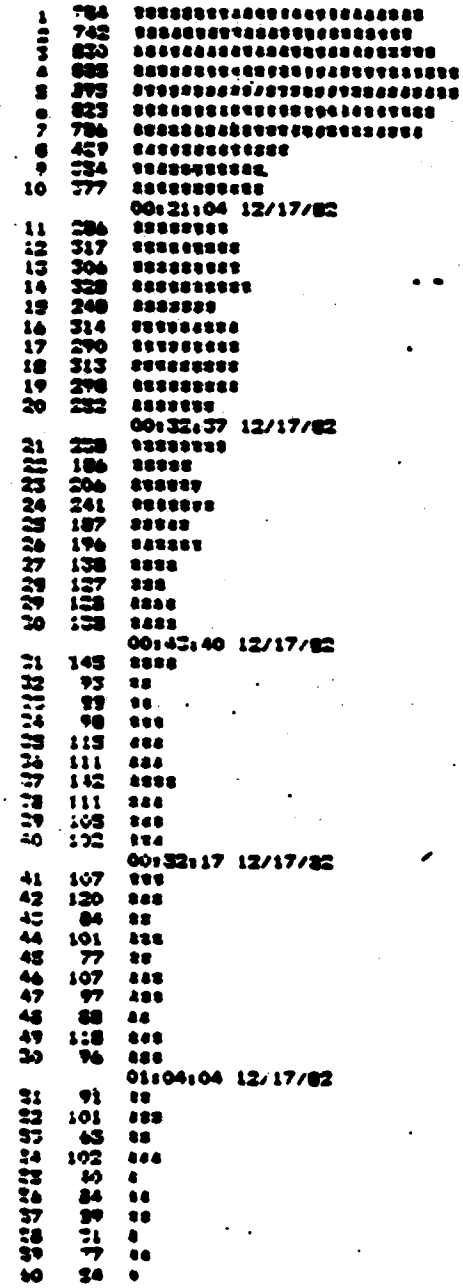

Fig. 3.3. Examples of low resolution output of 45° scattering cross section versus time as recorded by the laser nephelometer system as the NASA U-2 aircraft made a vertical ascent during one of the U-2 flights for NASA's Aerosol Climate Experiment during December 1983. As pointed out in the text, this parameter is approximately proportional to the total scattering cross section.

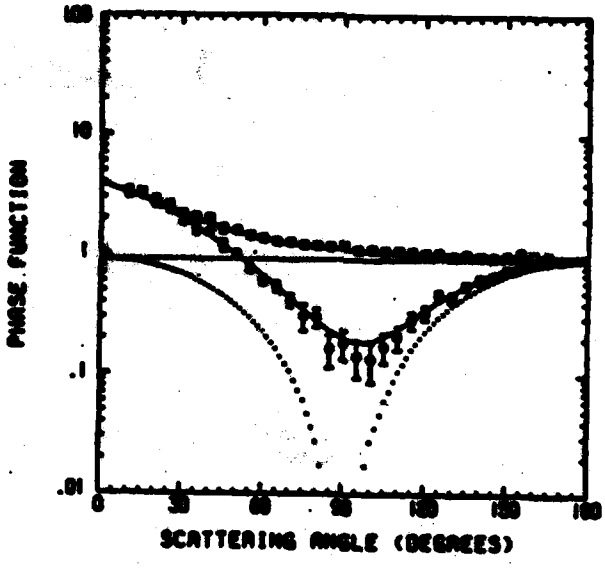

Fig. 3.4. Example of polar nephelometer observations for the stratospheric aerosol layer over Poker Flat, Alaska. The data were obtained on July 17, 1979. The squares are data points for scattering in the plane perpendicular to the electric vector of incident polarized light; the circles are data points for the parallel plane. Dotted lines are relative contributions to the phase functions due to molecular scattering; solid lines represent the phase function for both aerosol and molecular scattering using the Henyey-Greenstein phase function to specify the aerosol contributions. Best-fit Henyey-Greenstein parameters are an asymmetry parameter g = 0.52 and a ratio of aerosol to molecular scattering coefficient f = 0.65.

observed light-scattering pattern. Thus, relatively small errors in removing the molecular scattering contributions can seriously affect the inferences that one makes about the amount and angular distribution of light scattered by airborne particles. The second point to be made is the fact that the observed scattering patterns can usually be fit with the so-called Henyey-Greenstein phase function (Grams, 1981)

$$P_{HG}(\theta) = \frac{(1 - g^2)}{(1 + g^2 - 2g \cos \theta)^{3/2}}$$

in which g is the scattering asymmetry parameter and θ is the scattering angle. Figure 3.5 shows the form of these curves (dotted lines) for 3 cases ranging from g = 0.5 (bottom curve) to g = 0.7 (top curve). While the procedure described by Grams (1981) for obtaining "best-fit" Henyey-Greenstein parameters gives reasonable results for describing the scattering pattern for the sum of the aerosol and molecular components for cases in which the aerosols are relatively small contributors to the scattered light, cases involving heavy aerosol loading can cause complications for the analysis procedures and we found it necessary to search for a better approach.

At the present time, we believe that a modified version of the technique described by Grams (1981) will provide significantly better aerosol scattering cross sections. This technique takes advantage of the wide range of angles measured with the nephelometer device to provide a parameter that, in principle, completely eliminates contributions due to molecules. This procedure involves calculating for each forward angle the difference between the observation at that angle and the corresponding observation at the complementary angle. Thus, since the molecular scattering phase

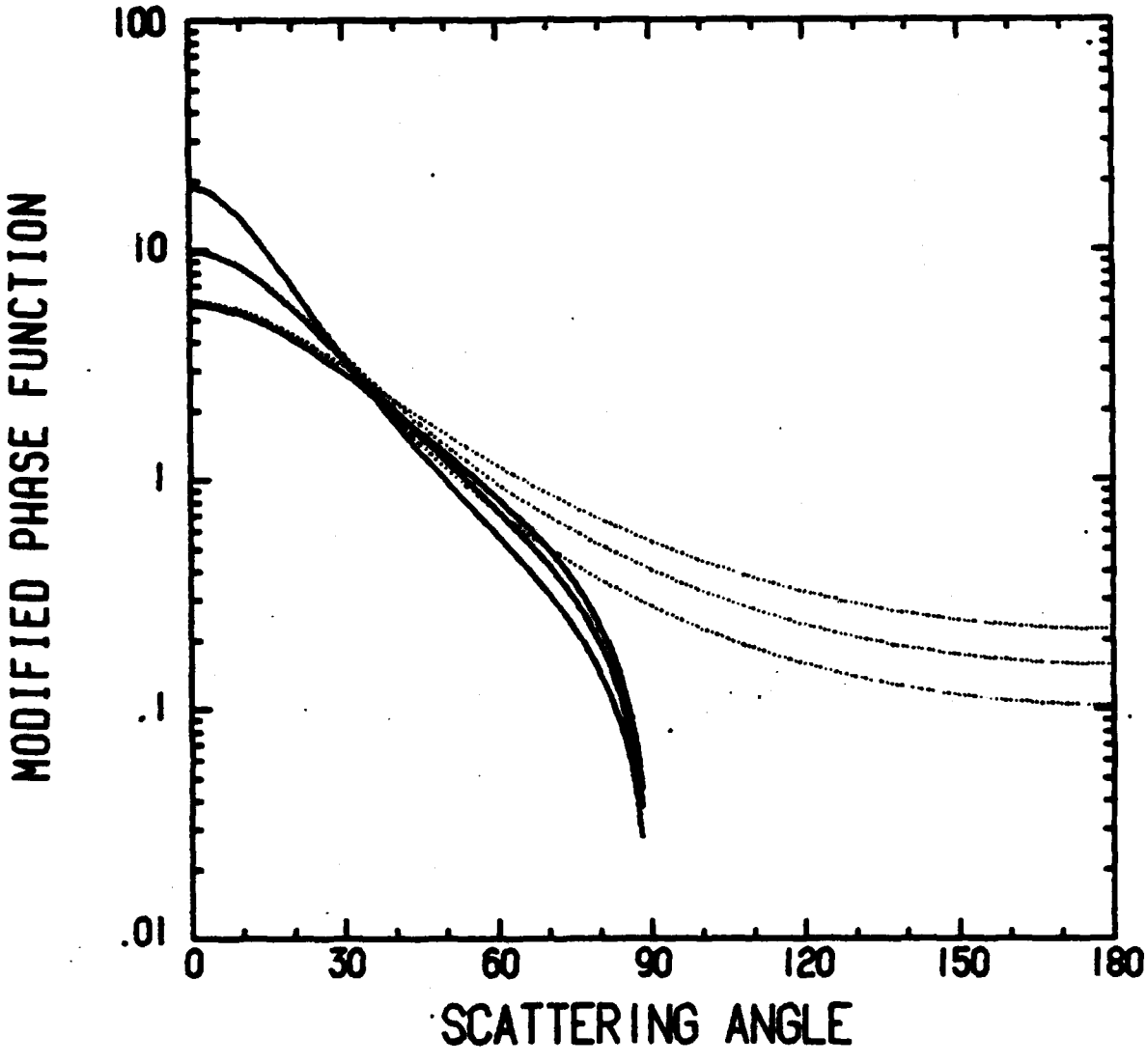

Fig. 3.5. Dotted lines are the Henyey-Greenstein phase functions for g = 0.5 (bottom line) to g = 0.7 (top line). Solid lines are the results of subtracting phase function values at complementary angles from values of the Henyey-Greenstein phase functions in the forward directions.

function is symmetric about 90°, the subtraction will remove all molecular contributions to the modified scattering parameter. The differences computed at each angle will then be directly proportional to aerosol concentrations and independent of the local molecular number density. The solid lines in Fig. 3.5 show the results of computing such differences for the Henyey-Greenstein phase functions. Note that for angles greater than about 40°, the curves are almost independent of the choice of the asymmetry parameter value. Our preliminary analysis, used to generate the scattering cross sections presented in this report, applies our least-squares curve-fitting programs to the problem of fitting the observations to the modified Henyey-Greenstein functions for angles between 40 and 90°, assuming g = 0.6 (which is typical of the "best-fit" asymmetry parameters obtained from our AGASP observations). This approach is a relatively recent development and further study is warranted. However, our preliminary analysis involving the use of Henyey-Greenstein phase functions indicates that the absolute values of the scattering cross-sections obtained by this approach should be accurate to within about 20%.

Figures 3.6 and 3.8 show the results of our analysis for two days of AGASP data - March 21 and March 31, 1983. Figures 3.7 and 3.9 show the corresponding analyses for condensation nuclei, ozone, aerosol extinction (integrating nephelometer), wind, temperature and dew point data obtained by other investigators on the same flights (Raatz et al., 1985). In subsequent discussions, we point out that the integrating nephelometer results are almost an order of magnitude higher than those calculated from the size distributions obtained with the particle sizing instruments on the AGASP flights. Our first comment on comparing our results with the other instruments is that the scattering cross sections obtained from the polar

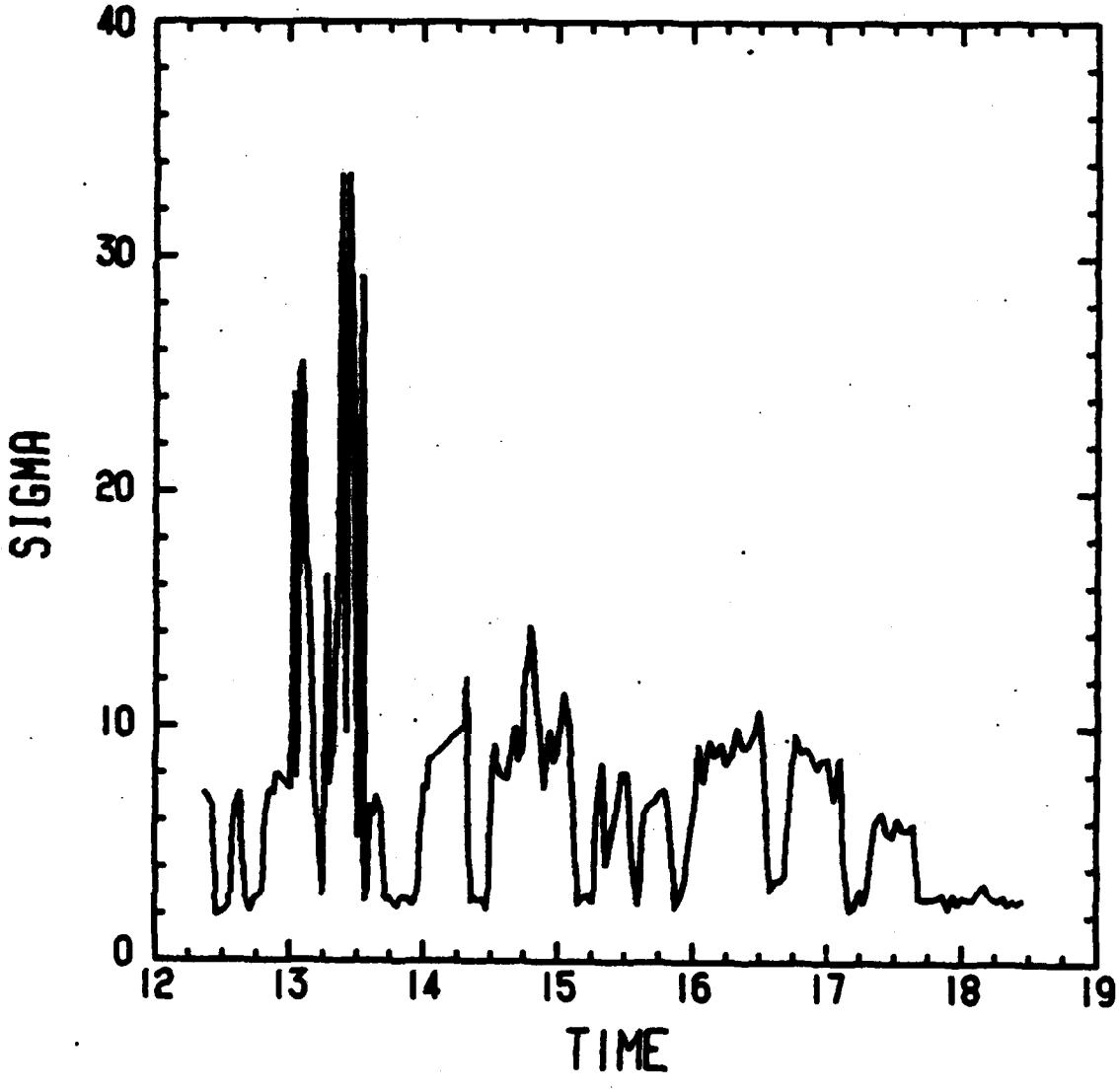

Fig. 3.6. Time series of scattering cross section (10^{-6}/meter) obtained by the polar nephelometer on March 21, 1983.

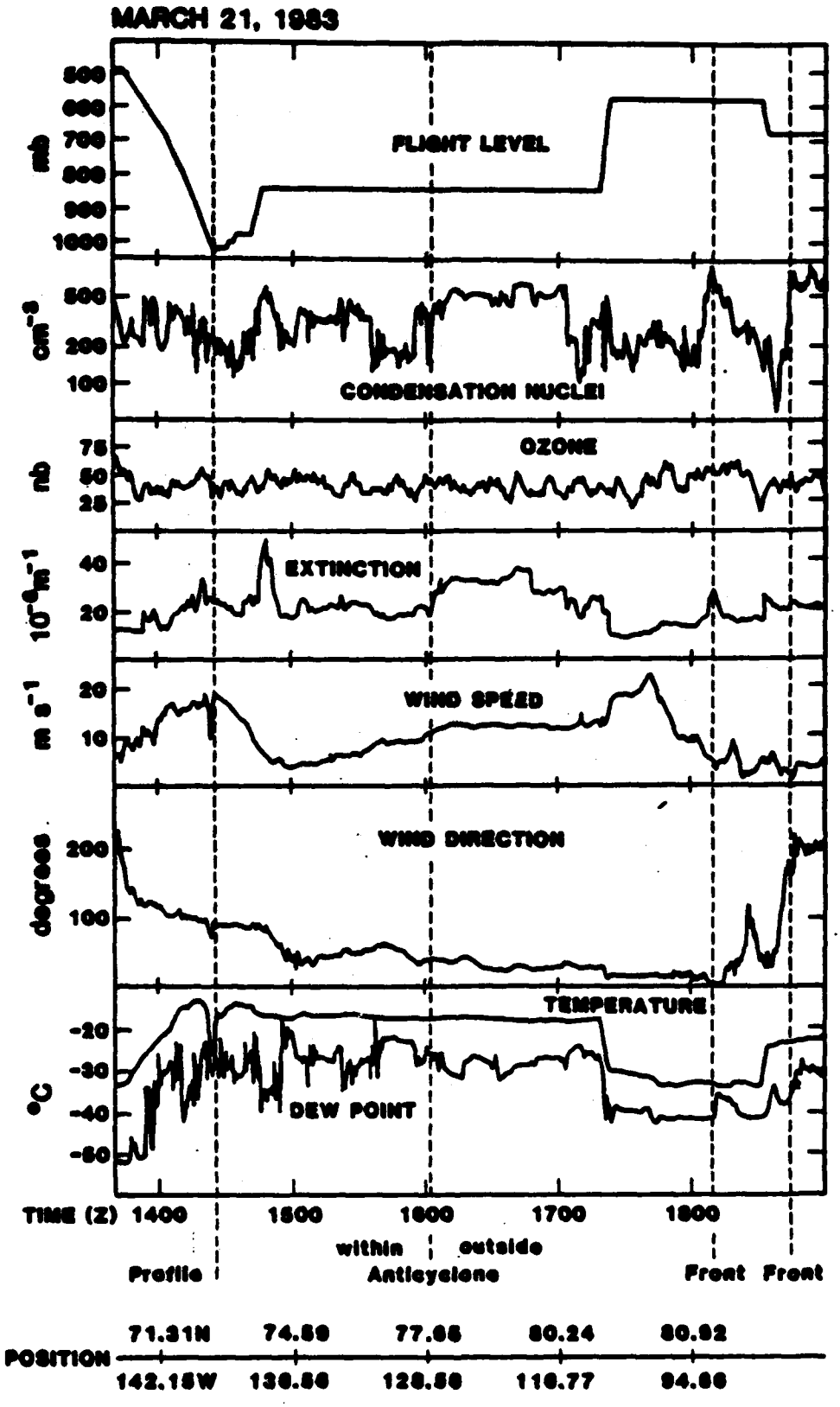

Fig. 3.7. Time series taken between 1340 (69.90°N, 143.85°W) and 1900 (78.33°N, 75.67°W) on March 21, 1983.

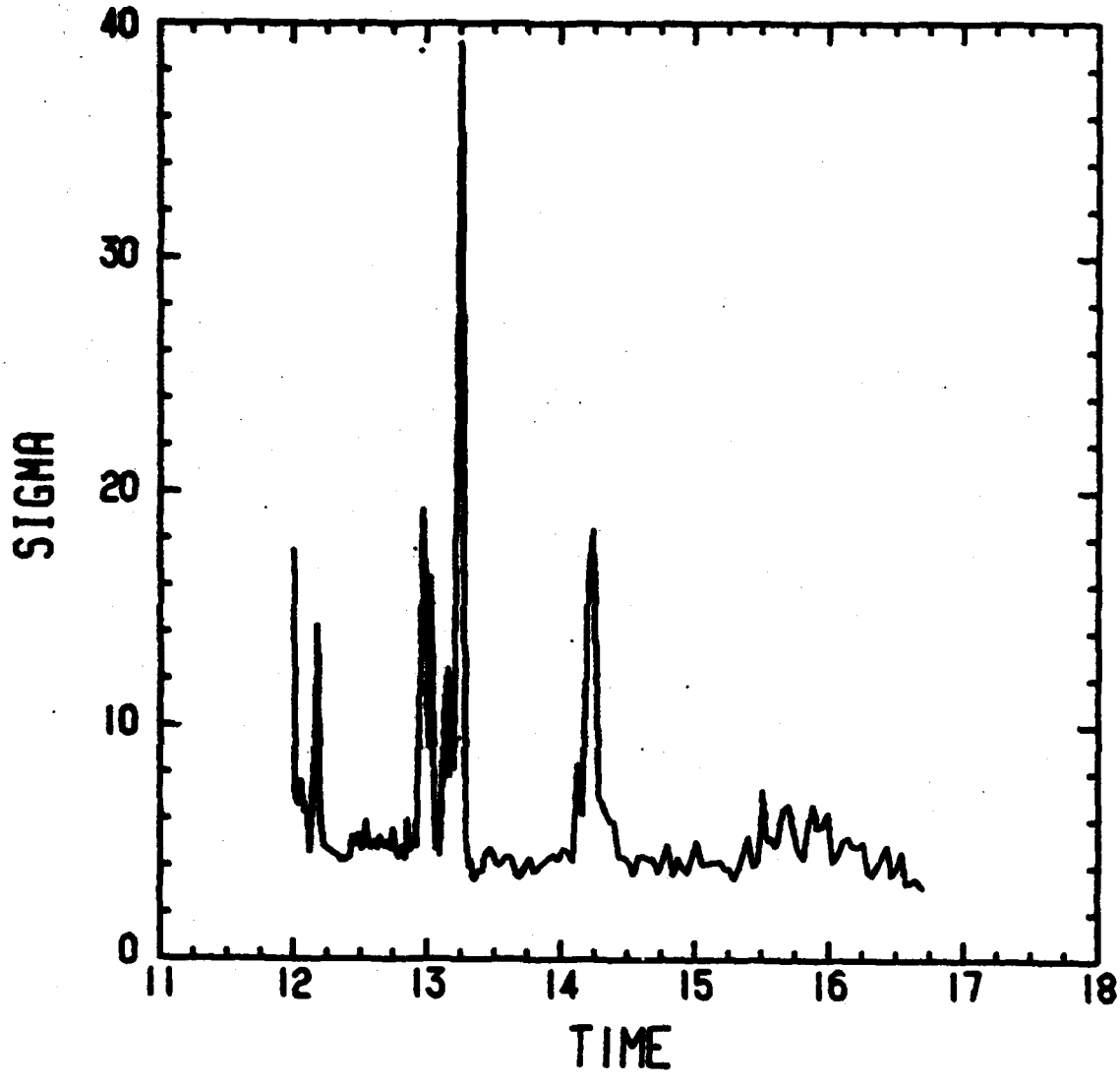

Fig. 3.8. Time series of scattering cross section (10^{-6}/meter) obtained by the polar nephelometer on March 31, 1983.

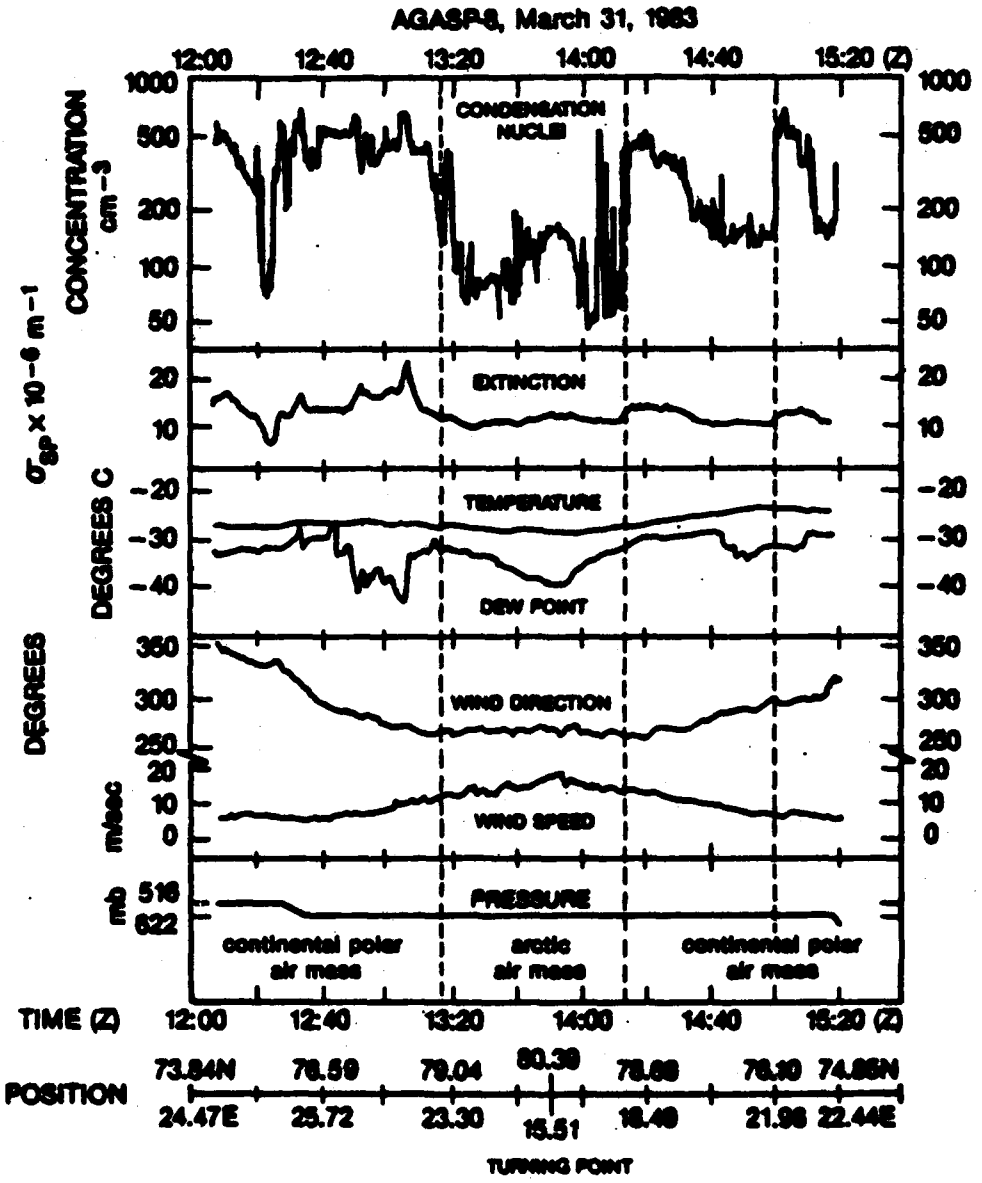

Fig. 3.9. Time series of aerosol and meteorological parameters for March 31, 1983, as the aircraft passed through an Arctic aerosol front at 620 mb (Raatz and Schnell, 1984).

nephelometer data are closer to those measured with integrating nephelometer. In most cases, the polar nephelometer values are somewhat smaller than those measured with the integrating nephelometer. However, in situations in which a high amount of variability in aerosol concentration is evident, the polar nephelometer appears to respond faster, increasing to relatively higher values than those recorded by the integrating nephelometer. The two different types of nephelometers do seem, therefore, to be in general agreement, although detailed comparisons often do tend to lead to some interesting differences. For example, at about 1810Z on March 21, Figs. 3.7 and 3.8 show a case in which the normal situation, as described above, is reversed; namely, the integrating nephelometer picked up a significant increase in aerosol extinction which was just barely detected by our instrument.

4. GENERAL ANALYSIS OF SIZE AND SCATTERING DATA

This analysis was primarily concerned with determination of best estimates of particle size for use in models of the radiative properties of the aerosol as well as for the interpretation of the scattering data. Among the areas of interest were the testing of the hypotheses incorporated in the Patterson et al. (1982) radiative models and the estimation of the radiative properties at infrared wavelengths. We have also identified some significant inconsistencies between two of the AGASP data sets. Although not an original goal, we have attempted to reconcile these two data sets, those of the integrating nephelometer and the PMS optical particle counters, and to understand the reasons for the inconsistencies.

Size Distributions - General Comparisons

The AGASP flights, other aircraft programs, and ground-based measurement programs in 1983 provided many different measurements of the aerosol size distribution under a variety of haze conditions. Consideration of a representative set of these measurements together with some earlier size distribution data can provide useful insight into the appropriate mode parameters for use in radiative modeling of the Arctic haze.

A comparison of the data is shown in Figure 4.1, which is a rather complex summary of the different size distributions. Each of the curves on this figure represent published data from measurements made during a spring aerosol maximum - either 1983 or a comparable earlier period (the Heintzenberg data). The published data have all been converted to dV/d log D distributions for consistency of presentation.

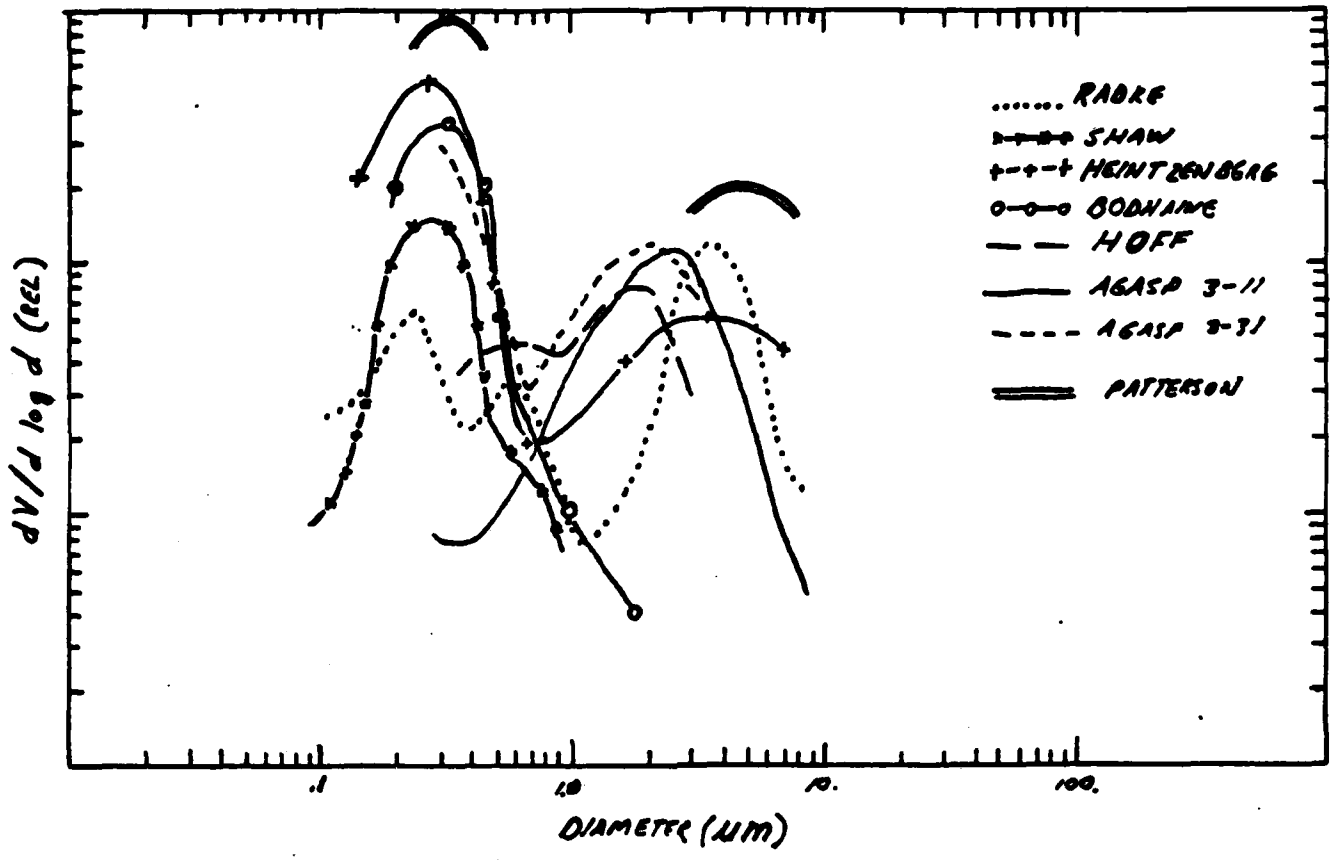

Fig. 4.1 Size distribution measurements of Arctic haze aerosols from a variety of sources plotted as dv/d log d distributions.

Two of the curves in the figure represent size distributions measured during AGASP flights(3-11-83, ——; 3-31-83, — —) [Schnell and Raatz, 1984; Raatz and Schnell, 1984]. The other curves show a size distribution measured over the Arctic Ocean by the University of Washington group (····) [Radke et al., 1984]; two 1983 size distributions measured at surface sites in Alaska, one at Barrow (o-o-o; Bodhaine, 1984) and one in central Alaska (*-*-*; Shaw, 1984); a size distribution measured at Spitzbergen by Heintzenberg (1980) (-+-+-+); and a size distribution measured in the Canadian Arctic (----) by Huff and Trivett.

We have also shown for comparison portions of the two modes used by Patterson et al. (1982) for their model of the Barrow spring maximum. These models of Patterson et al are shown displaced from the other modes for clarity.

Figure 4.1 shows quite clearly the overall modal structure of the Arctic haze aerosol. Each of the distributions which covers the submicron particle size range shows a submicron particle mode volume maximum between $\sim$ 0.2 and 0.3 μm diameter. Each of the distributions which covers the giant particle size range shows a peak in the 2 to 3 μm size range.

The 0.3 μm mode, which consists of sulfuric acid droplets as well as other secondary and combustion aerosols, is quite similar in mode characteristics to the accumulation mode measured in mid-latitude regions as discussed by Patterson et al. (1982) and to measurements made using microscopic analysis techniques (Biggs, 1980). The consistency in the different data sets for this accumulation mode indicates that we have a reasonable knowledge of the mode parameters of this major peak. Mie calculations indicate that the differences in the modes will not be significant when the calculations are normalized to measured scattering or extinction.

There is somewhat greater variability in observed mode parameters of the supermicron giant particle mode, but all of the data sets are consistent in indicating a mode volume maximum between 1.8 and 4 μm diameter. For these particles, the Patterson study inferred a mean radius somewhat larger than was generally observed during the AGASP flights, presumably due to longer transit times for these Arctic aerosols. Microscopic analysis (Rahn, 1978; Bailey et al., 1984) shows that giant particles consist in large part of crustal particles; ionic composition data of Radke (1984) suggest that there can be a significant sulfate and sea salt component for these larger particles as well. The exact composition of this giant particle mode will vary with location and time.

There is an additional feature in three of the data sets, those of Shaw, Schnell, and Radke, which is a mode or a shoulder near 0.7 μm diameter. The reason for this feature is not known, although the presence of the feature in three separate data sets suggests that it is not an artifact. In fact, Hoppel et al. (1985) report the presence of a similar mode in marine boundary layer data and discusses possible production mechanisms for such a mode.

While there is variation in the magnitudes of the modes and in the presence or absence of a 0.7 μm diameter particle mode, we can say that, in general, the broad features of the size distribution for the spring aerosol appear to be surprisingly well defined between 0.1 and 10 μm diameter. In addition, the similarity of these features to mid-latitude features confirms that the overall processes determining the size distribution can be understood in terms of similar mid-latitude processes, confirming the inferences of Patterson et al.

Size Distributions - AGASP Data

Because of the ability to make detailed comparisons with the optical and the chemical data, including the integrating and polar nephelometer data, we have emphasized interpretation of the size data obtained during the AGASP program.

The real-time size distribution measurements aboard the WP-3D during the AGASP flights were made with two externally mounted PMS aerosol probes, an ASASP-100X for smaller particles (those with d < 3 μm) and an FSSP for larger "giant" particles (those with diameters between 3 and 10 μm). Analysis has shown that both probes are needed to measure particle size for radiatively important particles.

Six representative measurements of the aerorol size distributions are shown in Figs. 4.2a, 4.2b, and 4.2c. The figures include ASASP-100X data (•) and FSSP data (o); the presentation is in the form of number concentration as well as mass concentration versus size. The plots in Figs. 4.2a and 4.2b represent data in the Alaskan Arctic; the plots in Fig. 4.2c represent data in the European Arctic.

It is apparent that in these, as in the other data sets, the aerosol exhibits a bimodal structure. The mode with a mass peak near 2 μm is well defined. Because of some problems with the ASASP probe, the first three channels of data were not used in the analysis. Consequently, the data extend only to ∿ 0.3 μm diameter and are not sufficient to determine mode parameters for the submicron mode. On the basis of aerosol microphysics as well as the other Arctic measurements discussed above, we can infer that the mass peak is near 0.3 μm diameter. This assumption is not inconsistent with the PMS optical particle counter data.

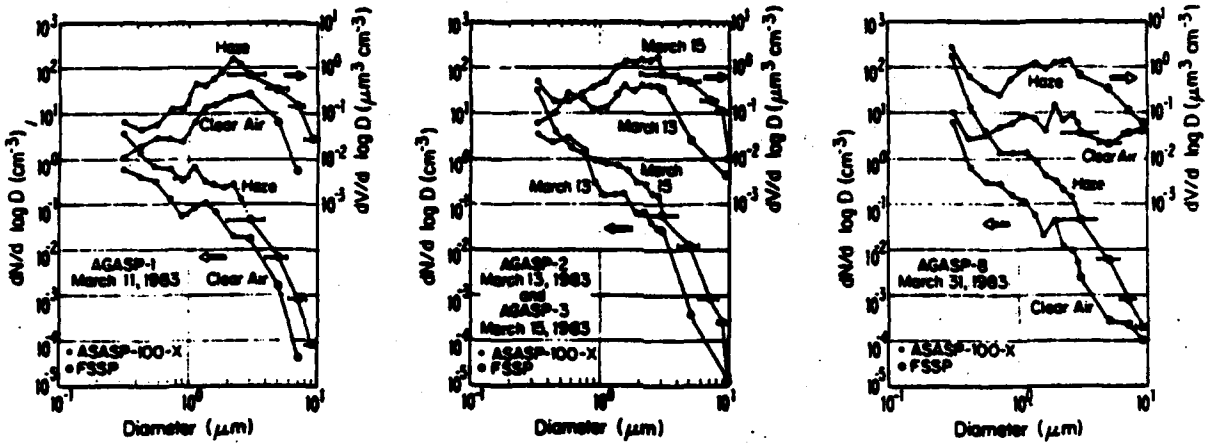

Fig. 4.2 Aerosol concentration and mass spectra for Arctic haze aerosols. 4.2a includes haze and clear air data for AGASP-1 on March 11, 1983; 4.2b includes data from AGASP-2 and AGASP-3; 4.2c includes data from AGASP-8. More details on collection times and altitudes are available in the original sources for the figures [from Schnell and Raatz, 1984(a&b) and Raatz and Schnell, 1984(c)].

Previous work has shown that aerosol size distributions can generally be represented by a log-normal distribution of the form

$$\frac{dN}{d \log r} = \frac{N_o}{\sqrt{2\pi} \log \sigma} \exp - [\frac{(\log r - \log ro)^2}{^2\log\ ^2\sigma}]$$

in which N_o is the total particle number, r_o is the number mean radius, and σ is the parameter, the standard deviation, which describes the width of the distribution. For the log-normal distribution, the volume distribution has the same form as the number distribution, and the volume mean radius is related to the number mean radius by the equation

$$\ln r_v = \ln r_N + 3 \ln^2\sigma \quad .$$

The mass distribution may be determined by multiplying the volume distribution by the appropriate particle density. The radius terms may be replaced with diameter terms in either of the equations.

We have made approximate log-normal fits to the giant particle mode centered near 3 μm on the volume distributions. Although there were minor differences in mode parameters in each case, an adequate fit for all of the distributions was obtained with d_N value of 1 μm and a σ of 1.75, with a corresponding d_v value of 2.6 μm. We see that both the European Arctic and the Alaskan Arctic data show a striking similarity in mode parameters. This suggests that these giant particles are representative of a well aged aerosol that has been transported a long distance.

The data suggest a good deal of variability in the submicron particle mode. The data as presented in Figs. 4.2a, b, c suggest that the giant particles are relatively more important in producing the radiative effects

of the aerosol that we would expect on the basis of other data sets. This is not the case, however, as we will see in the next section, since a more detailed analysis of the PMS data set indicated some problems in the data, particularly with regard to the submicron mode concentration and sizing.

Size and Optical Scattering Measurements - A Comparison

The validity of an individual data set may be tested by means of intercomparisons among simultaneous data sets. The large number of simultaneous measurements of aerosol parameters measured in AGASP allows us to make such detailed intercomparisons among the measurement sets. One such intercomparison involves the PMS data and the simultaneous integrating nephelometer data. In this comparison the PMS size distributions presented by Raatz and Schnell were used to calculate the scattering expected for the aerosol for a wavelength of 0.55 μm, the approximate wavelength of the integrating nephelometer. Separate calculations were made for the submicron and the giant particle modes; nominal optical properties (Patterson et al., 1982) were used for both the giant and the submicron particle mode calculations. As a first cut, because of the uncertainties of fitting a log-normal distribution to the submicron PMS data, this submicron data was approximated by a Junge distribution extending from a diameter of 0.2 μm to 1 μm. The results of this calculation for scattering are shown in Table 4.1; simultaneous integrating nephelometer data are also shown in Table 4.1.

It is apparent from the data in Table 4.1 that there is a serious discrepancy between the optical scattering inferred from the AGASP PMS data and the nephelometer scattering data, with the calculated scattering less than the observed scattering by an order of magnitude or more. The polar nephelometer data, although somewhat lower than the integrating nephelometer data, show the same discrepancy.

TABLE 4.1

PMS DISTRIBUTION SCATTERING CALCULATIONS

DATE	HAZE[+] CONDITION	SCATTERING CALCULATIONS FOR $\lambda = .55$ μm (m^{-1})			INTEGRATING NEPHELOMETER SCATTERING
		Submicron	Giant	Total	
3-11[1]	H	0.2×10^{-6}	0.9×10^{-6}	1.1×10^{-6}	20×10^{-6}
3-11[1]	C	0.1×10^{-6}	0.2×10^{-6}	0.3×10^{-6}	11×10^{-6}
3-13[1]	H	0.8×10^{-6}	0.4×10^{-6}	1.2×10^{-6}	15×10^{-6}
3-15[1]	H	1.6×10^{-6}	1.8×10^{-6}	3.4×10^{-6}	20×10^{-6}
3-31[2]	H	5.1×10^{-6}	3.1×10^{-6}	8.2×10^{-6}	15×10^{-6}
3-31[2]	C	0.2×10^{-6}	0.3×10^{-6}	0.5×10^{-6}	10×10^{-6}

[+]H = Haze, C = Clear

[1]Schnell and Raatz (1984)

[2]Raatz and Schnell (1984)

TABLE 4.2

MODIFIED SCATTERING CALCULATIONS

DATE	HAZE+ CONDITIONS	SCATTERING CALCULATIONS FOR λ = .55 μm (m^{-1})			INTEGRATING NEPHELOMETER SCATTERING
		Submicron	Giant	Total	
3-11[1]	H	8.8×10^{-6}	0.9×10^{-6}	9.7×10^{-6}	20×10^{-6}
3-11[1]	C	1.7×10^{-6}	0.2×10^{-6}	1.9×10^{-6}	11×10^{-6}
3-13[1]	H	17.8×10^{-6}	0.4×10^{-6}	20.2×10^{-6}	15×10^{-6}
3-15[1]	H	7.7×10^{-6}	1.8×10^{-6}	9.5×10^{-6}	20×10^{-6}
3-31[2]	H	11.0×10^{-6}	3.1×10^{-6}	14.1×10^{-6}	15×10^{-6}
3-31[2]	C	3.3×10^{-6}	$.3 \times 10^{-6}$	3.6×10^{-6}	10×10^{-6}

+H = Haze, C = Clear

[1]Schnell and Raatz (1984)

[2]Raatz and Schnell (1984)

TABLE 4.3

10.6 μm EXTINCTION DATA

DATE	HAZE CONDITION	CALCULATED EXTINCTION (m^{-1})		
		Submicron	Giant	Total
3-11-83	Haze	2.4×10^{-7}	2.1×10^{-7}	4.5×10^{-7}
3-11-83	Clear	$.5 \times 10^{-7}$	$.4 \times 10^{-7}$	0.9×10^{-7}
3-13-83	Haze	5.4×10^{-7}	$.8 \times 10^{-7}$	6.2×10^{-7}
3-15-83	Haze	2.1×10^{-7}	4.0×10^{-7}	6.1×10^{-7}
3-31-83	Haze	3×10^{-7}	6.9×10^{-7}	9.9×10^{-7}
3-31-83	Clear	$.9 \times 10^{-7}$	$.5 \times 10^{-7}$	1.4×10^{-7}

The integrating nephelometer data may also be comapred with the direct radiative mesurements of Valero et al. (1983) for March 31, 1983. Valero measured upward and downward flux at several wavelengths. Ackerman and Valero (1984) used this flux data and assumed nominal aerosol properties to estimate an optical depth of $\sim$ 0.3 for the haze layers at mid-visible wavelengths. By comparison, an approximate integration of the integrating nephelometer data with altitude suggests an optical depth due to scattering of about .13, roughly half of the total optical depth inferred by Ackerman and Valero. Although the numbers are not entirely consistent, the comparison does indicate that the nephelometer is measuring scattering that is not grossly in error.

A further comparison of observed volume concentrations of the submicron particle mode with mass concentrations of carbon and sulfur (which are primarily associated wtih the submicron mode) presented by Hanson and Rosen, 1984 for the March 11 and March 13 flights indicates that the PMS data significantly underestimates the amount of material present in the small particle mode, possibly by a factor of 4 or more. These comparisons suggest very clearly that the PMS data represents a significant underestimation of the actual aerosol concentrations.

The lack of small particle data and the possibility of response differences in the PMS probes between the calibration aerosol and the measured aerosol (see e.g., Pinnick et al., 1983 for discussion) in the 0.3 - 0.5 μm size range suggest that the discrepancy may be primarily in the smaller size particles. We have tested this possibility by assuming that the actual submicron size distribution is an average size distribution that is determined from the curves on Fig. 4.1. We have used the Shaw data from the figure to fit a log-normal distribution with a d_N of

0.17 μm a d_v of .28 μm and a σ of 1.46. The appropriate particle number for the distribution is assumed to be given by the total particle number measured with the condensation nucleus counter aboard the WP-3D aircraft for the time period in question.

The results of these new calculations are shown in Table 4.2. It is apparent that the discrepancy between calculated and measured scattering has been significantly reduced. This indicates that the assumption that the PMS probes underestimate the small particle concentration is a valid one. We infer that a size distribution determined by combining an average submicron size distribution that is matched to the measured particle number with the measured giant particle size distribution is adequate as a first approximation to the actual size distribution.

An example of such a modified size distribution in shown in Figure 4.3. We can see in the figure that the PMS optical particle counter data appear to underestimate our inferred particle number in the 0.3 - 0.5 μm size range. This may be explained with reference to data of Pinnick and Auvermann (1979) who have shown that the ASASP probes will underestimate the particle size in this size range if the particle is highly absorbing relative to the calibration aerosol. The Arctic aerosol is known to be absorbing and the real component of the refractive index is less than that of the polystyrene latex spheres. We would expect then that the measured particles are larger than indicated, which would have the effect of increasing the maximum size, reducing the logarithmic width of the size range, and causing the dV/d log d plot to be higher than indicated. This would result in a greater consistency between the inferred and the measured distributions.

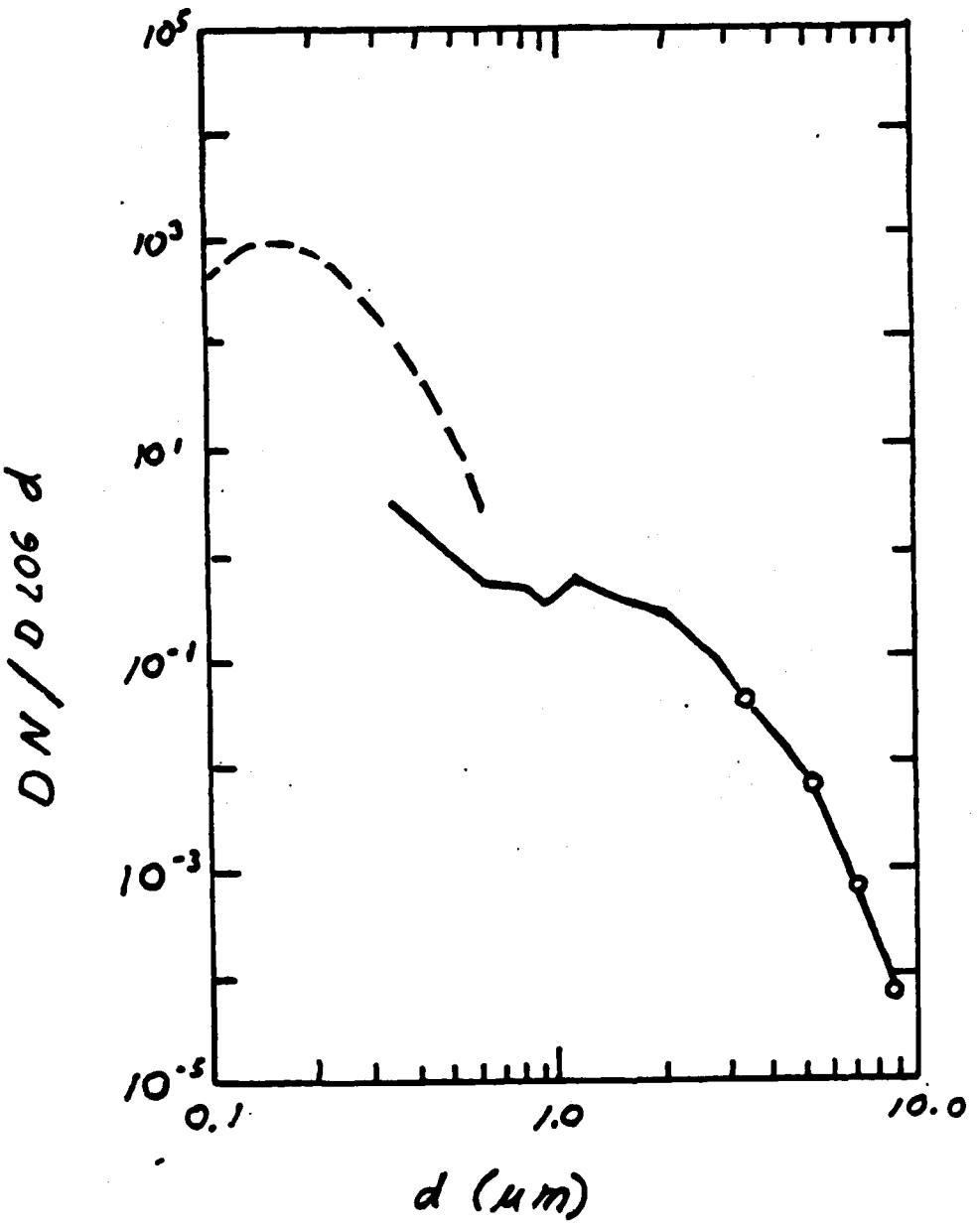

Fig. 4.3 Assumed submicron particles size distributions (——) and PMS determined size distribution (————) for the AGASP-I haze data.

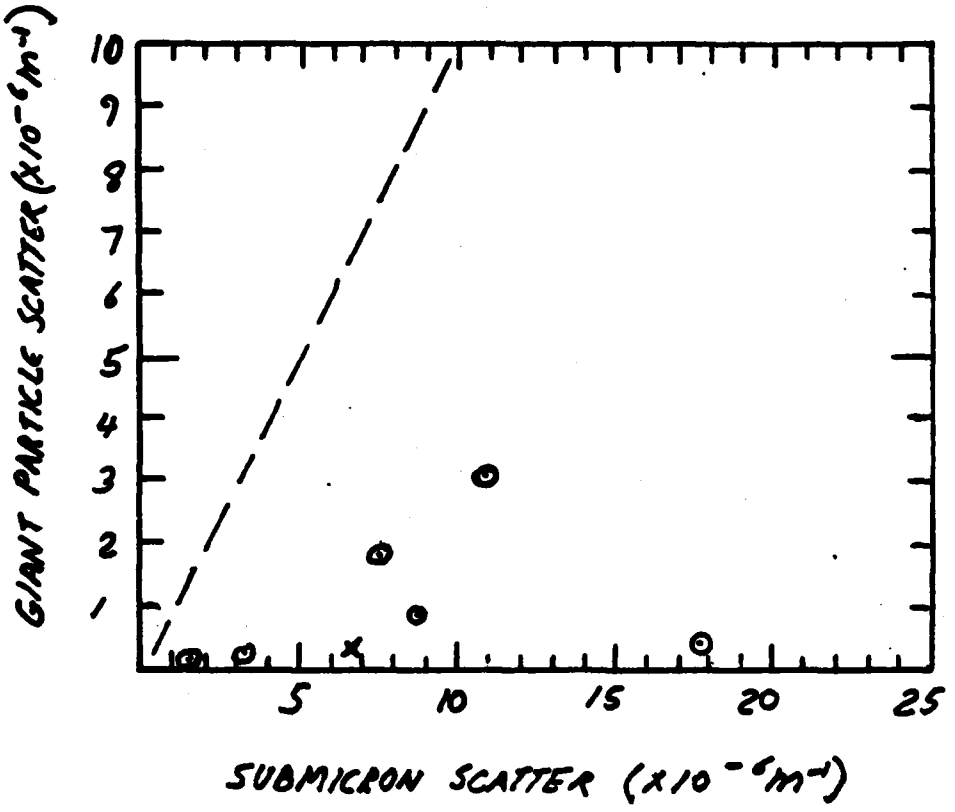

Fig. 4.4 Inferred giant and submicron scattering for the AGASP data (•) and for the Radke et al. (1984) haze data. The figure confirms the importance of the submicron mode.

Inferences from Size and Scattering Data

The purpose of this section is to use our size data, as modified to conform with the scattering data, to give an estimate of the relative importance of submicron and giant particles in producing visible wavelength radiative effects and to determine the extinction of the aerosol at 10.6 μm as an estimation of the magnitude of the infrared effects.

We have used our modified size distribution to calculate scattering for both submicron and giant particles. The results for each of the AGASP samples, and for the Radke data, are shown in Fig. 4.4a. The modified AGASP data is consistent with the Radke data in confirming that the giant particle mode is of little importance in producing visible wavelength effects in haze situations.

The mid-infrared effects are expected to be much more heavily influenced by the giant paritcle mode and this is confirmed by the data of Table 4.3 which shows the extinction of 10.6 μm due to both submicron and giant particle modes for each of the data sets, as well as the total extinction. These data were calculated using the urban aerosol refractive index data of Shettle and Fell (1979) for the submicron particles; the giant particle refractive index was assumed to be 1.7 - .3i, a value appropriate to soil particles as discussed by Patterson (1981).

The calculated values for the 10.6 μm extinction in haze layers range from .4 x $10^{-7}m^{-1}$ to 0.9 x $10^{-7}m^{-1}$; possible variations in the submicron particle concentration will have an effect on the calculated extinction, but the effect is less significant than at visible wavelengths. Those 10.6 μm extinction values are somewhat more than an order of magnitude less than the visible wavelength values. The infrared effects are of

potential importance, however, because the effects can persist throughout the polar winter night while the visible wavelength effects are of importance only in a relatively short period of time in the spring. The possible importance of these infrared effects will have to be determined by appropriate modeling efforts.

Because of the importance of the absorption in determining the infrared effects, knowledge of the imaginary component of the refractive index is crucial in determining these effects. There is, however, considerable uncertainty in the appropriate values to use since there are no direct measurements of the Arctic haze giant particles. If the modeling efforts do show that the infrared effects are significant, then better determinations of the infrared properties, absorption properties in particular, will be needed.

5. CONCLUSIONS

We have analyzed the polar nephelometer data to determine aerosol scattering cross sections. We have also used scattering and aerosol microphysical data to improve estimates of aerosol properties for radiative modeling. We have confirmed earlier estimates of the submicron size distribution and have shown that size measurements are consistent in indicating a mass peak at $\sim$ 0.3 μm diameter. The size distributions appear to be adequately represented by log-normal distributions with a standard deviation of $\sim$ 1.5. The data in general indicate the importance of the submicron accumulation mode in producing optical effects at solar wavelengths.

We have shown that the giant particles as measured during MONEX have relatively uniform distributions characterized by a volume peak at $\sim$ 2.5 μm diameter, a size somewhat smaller than previously inferred by Patterson et al.

We have also used a comparison of several data sets to indicate some inconsistencies in the data and to discuss the reasons for the inconsistencies. We have been able to point out some deficiencies in the optical particle counter data.

We have plans for future work with the nephelometer data to explore AGASP data in more detail. For the purposes of supporting the conclusions of this report, however, we wish only to point out our new approach for analyzing the polar nepheloemter data appears to offer a considerable amount of promise for future aerosol studies. It clearly offers a more accurate procedure for establishing an absolute value for the optical cross section of the aerosol particles by eliminating problems associated with trying to establish the local number density to remove the Rayleigh

scattering cross section from each observation of the atmospheric volume scattering cross section. Furthermore, the ability to establish an accurate value of the aerosol scattering contribution allows one to calculate the ratio of aerosol to molecular scattering which was one of the variables obtained in the least-square curve fitting procedure described by Grams (1981). The elimination of the need to produce an estimate of this variable will significantly increase the speed and reliability of the procedure that we used in the past for analyzing the nephelometer results.

6. REFERENCES

Ackerman, T.J. and Valero, F.P.J. (1984). The vertical structure of Arctic haze as determined from airborne net-flux radiometer measurements. Geophys. Res. Lett., 11, 469-472.

Bailey, I.H., Radke, L.F., Lyons, J.H. and Hobbs, P.V. (1984). Airborne observations of Arctic aerosols, 2, Giant Particles. Geophys. Res. Lett., 11, 397-400.

Bigg, E.K. (1980). Comparison of the aerosol at four baseline atmospheric monitoring stations. J. Appl. Met., 19, 521-533.

Bodhaine, B.A., Dutton, E.G. and DeLuisi, J.J. (1984). Surface aerosol measurements at Barrow during AGASP. Geophys. Res. Lett., 11, 377-380.

Grams, G.W. (1981). In-situ measurements of scattering phase functions of stratospheric aerosol particles in Alaska during July 1979. Geophys. Res. Lett., 8, 13-14.

Grams, G.W. and A. Coleeti (1982). Analysis of polar nephelometer data obtained at the First International Workshop on Light Absorption by Aerosol Particles. In Light Absorption by Aerosol Particles (H.E. Gerber and E.E. Hindman, Eds.), Spectrum Press, Hampton, Virginia.

Grams, G.W. (1983). In-situ light scattering techniques for determining aerosol size distributions and optical constants. Final Report, U.S. Army Research Office Contract Number DAAG29-79-C-0092, School of Geophysical Sciences, Georgia Tech, Atlanta, Georgia.

Grams, G.W., Dascher, A.J., and Wyman, C.M. (1975). Laser polar nephelometer for airborne measurements of aerosol optical properties. Optical Eng., 14, 85-90.

Hansen, A.D.A. and Rosen, H. (1984). Vertical distribution of particulate carbon, sulfur and bromine in the Arctic haze and comparison with ground level measurements at Barrow Alaska. Geophys. Res. Lett., 11, 381-394.

Hoppel, W.A., Fitzgerald, J.W. and Larson, R.E. (1985). Aerosol size distributions in air masses advecting off the east coast of the United States. J. Geophys. Res., 90, 2365-2379.

Hoff, R.M. and Trivett, N.B.A. (1984). Ground-based measurements of Arctic haze made at Alert, N.W.T., Canada during the Arctic Gas and Arctic Sampling Project (AGASP). Geophys. Res. Lett., 11, 389-392.

Patterson, E.M. (1981). Optical properties of the crustal aerosol: relation to chemical and physical characteristics. J. Geophys. Res., 86, 3236-3246.

Patterson, E.M., Marshall, B.T. and Rahn, K.A. (1982). Radiative properties of the Arctic aerosol. Atmos. Environ., 16, 2967-2977.

Pinnick, R.G. and Auvermann, J.J. (1979). Response characteristics of Knollenberg light-scattering aerosol counters. J. Aerosol Sci., 10, 55-74.

Raatz, W.E. and Schnell, R.C. (1984). Aerosol distribution and an Arctic front during AGASP: Norwegian Arctic. Geophys. Res. Lett., 11, 373-376.

Rahn, K.A., Borys, R.D., Shaw, G.E. and others (1979). Long range impact of desert aerosols on atmospheric chemistry: Two examples. in Morales, C., ed., Saharan Dust: Mobilization, Transport, Deposition: SCOPE 14, Chichester, Wiley and Sons, pp.243-266.

Schnell, R.C. (1984). Arctic haze and the Arctic Gas and Aerosol Sampling Program (AGASP). Geophys. Res. Lett, 11, 361-364.

Schnell, R.C. and Raatz, W.E. (1984). Vertical and horizontal characteristics of Arctic haze during AGASP: Alaskan Arctic. Geophys. Res. Lett., 11, 369-372.

Shaw, G.E. (1984). Microparticle size spectrum of Arctic haze. Geophys. Res. Lett., 11, 409-412.

Shettle, E.P. and Fenn, R.W. (1979). Models for the Aerosols of the Lower Atmosphere and the Effects of Humidity Variations on their Optical Properties. Technical Report AFGL-TR-79-0214 Air Force Geophysics Laboratory, Hanscom AFB, MA 01731.

Valero, F.P.J., Ackerman, T.P. and Gore, W.J.Y. (1983). Radiative effects of the Arctic haze. Geophys. Res. Lett., 10, 1184-1187.

PUBLICATIONS SUPPORTED BY THIS GRANT

Publications based on Work Directly Supported by this Grant:

Patterson, E.M. (1985): Aerosol Size Distributions in the Arctic Haze - Similarities and Differences Among Data Sets and Implications for Radiative Transfer Calculations. to be submitted to Atmospheric Environment.

Publications based on Work Indirectly Supported by this Grant:

Patterson, E.M. and Grams, G.W. (1984): Absorption and Scattering in the Free Troposphere in Proceedings of the 1985 International Radiation Symposium, G. Fiocco, ed., to be published by Spectrum Press, Hampton, VA.

PARTICIPATING SCIENTIFIC PERSONNEL

Principal Investigator: E. M. Patterson

Professional Personnel

A. Coletti (Research Scientist)
C. M. Wyman (Research Technologist)
G. W. Grams (Professor)

END

FILMED

9-85

DTIC